Exciton Band Topology in Spontaneous Quantum Anomalous Hall Insulators: Applications to Twisted Bilayer Graphene

Yves H. Kwan[⬤],[*] Yichen Hu, Steven H. Simon, and S. A. Parameswaran[⬤]
Rudolf Peierls Centre for Theoretical Physics, Clarendon Laboratory, Oxford OX1 3PU, United Kingdom

We uncover topological features of neutral particle-hole pair excitations of correlated quantum anomalous Hall (QAH) insulators whose approximately flat conduction and valence bands have equal and opposite nonzero Chern number. Using an exactly solvable model we show that the underlying band topology affects both the center-of-mass and relative motion of particle-hole bound states. This leads to the formation of topological exciton bands whose features are robust to nonuniformity of both the dispersion and the Berry curvature. We apply these ideas to recently reported broken-symmetry spontaneous QAH insulators in substrate aligned magic-angle twisted bilayer graphene.

Introduction.—The structure of the ground states of condensed matter systems intricately affects their low-temperature properties, and is imprinted in the spectrum of low-energy quasiparticles and long-wavelength collective excitations. Electrical insulators generically break no continuous symmetries and hence lack gapless collective modes, and are gapped to charge transport in their bulk. However, interactions can stabilize neutral excitons, bound states of a hole in the valence band, and an electron in the conduction band. While also gapped, excitons typically have lower energy than charged excitations and dominate the optical response of direct-gap semiconductors, where they can be excited at zero wave vector. More generally, excitons form at a fixed "center of mass" (CM) wave vector $\boldsymbol{q}$ set by the momentum separation between the valence band maximum and conduction band minimum. The spectrum and transport properties of excitons can also be modified by the topology of the electronic bands near these extrema [1,2]. This is captured by the *excitonic* Berry curvature [3] linked to the evolution of the two-particle bound state across its Brillouin zone (BZ). Such considerations are relevant, for example, to two-dimensional transition-metal dichalcogenides [4], where the valley-contrasting anomalous velocity of excitons has been experimentally observed [5].

Here, we focus on excitons in correlated insulators formed in moiré heterostructures of twisted bilayer graphene (TBG) aligned with hexagonal boron nitride (*h*-BN). In the "magic-angle" regime, absent interactions, the relevant band structure has a gapped Dirac dispersion with four degenerate bands below and above charge neutrality [6,7]. Members of each degenerate quartet are labeled by spin ($\sigma = \uparrow, \downarrow$) and valley ($\tau = \pm$) indices. The valleys correspond to the $\pm K$ points of the single-layer BZ, have Chern numbers $C = \tau$, and are interchanged by time-reversal symmetry (TRS). At integer filling, the suppressed bandwidth ($\lesssim 10$ meV) allows interactions to stabilize TRS-breaking valley- and spin-polarized states in which a partial subset of the bands is fully occupied—a mechanism proposed to explain the observed quantized anomalous Hall (QAH) response in *h*-BN TBG [8].

We identify several striking features of the exciton spectrum in *h*-BN TBG linked to the flatness and nontrivial Chern number of the underlying single-particle bands coupled with the spontaneous breaking of time-reversal and spin rotation symmetries. We root our understanding of universal topological features in an analytically tractable model that mimics the features of the *h*-BN TBG band structure by leveraging the mapping between $|C| = 1$ Chern bands and Landau levels (LLs). Our four-band model has perfectly flat dispersion and uniform Berry curvature, and consists of spinful electron LLs whose Chern number has a sign set by a twofold degenerate valley index. We examine excitations of a fully spin-and-valley-polarized state with one filled LL. We show that the intravalley spin-wave mode has the gapless quadratic dispersion expected for Goldstone modes of a conserved order parameter, consistent with closely related quantum Hall ferromagnets [9,10]. In striking contrast, we show that the intervalley excitonic bands of our model are gapped and exactly flat. The flatness of the bands admits low-energy $\boldsymbol{q} = 0$ excitons throughout the BZ, and also leads us to consider the dynamics of the excitonic CM which is conjugate to $\boldsymbol{q}$. Strikingly, we find that the CM motion experiences significant anomalous velocity, linked to the Berry curvature of the evolution of the particle-hole (PH) pair wave function as $\boldsymbol{q}$ evolves across the CM. We demonstrate that these qualitative features survive the introduction of finite bandwidth and Berry curvature inhomogeneity, and discuss the results in a microscopic model of *h*-BN TBG. Our work illustrates that correlated ground states in moiré heterostructures can host unconventional excitations, whose many-body physics we explore elsewhere [11].
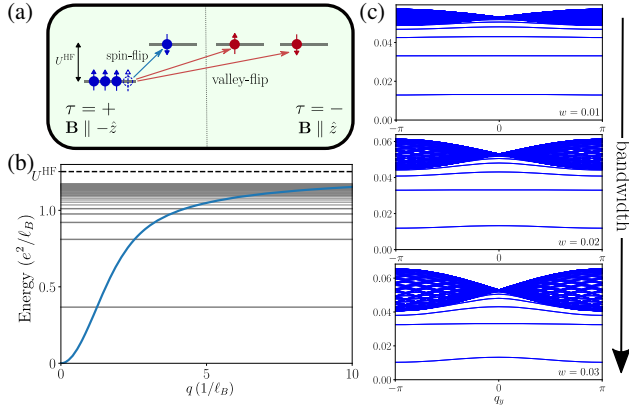
FIG. 1. (a) Schematic of the four-band LLL model at $\nu = 1$ showing the exchange-splitting $U^{\mathrm{HF}} = \sqrt{(\pi/2)}(e^2/\ell_B)$ and the different neutral excitation types. (b) Spin wave energy (blue curve) as a function of y-momentum q for $\alpha = 0$. Horizontal lines show the momentum-independent valley-flip exciton energies. Both modes saturate to U^{HF}. (c) Intervalley exciton spectrum at $q_x = 0$ in the magnetic Brillouin with increasing bandwidth $w = 0.01, 0.02, 0.03$. Calculations were performed on a 20×20 momentum-space mesh.

Exactly solvable model.—We exploit the topological equivalence between $|C| = 1$ Chern bands and LLs, and consider a system of four flavors of electronic LLs confined to the plane [Fig. 1(a)]. The two valleys $\tau = \pm$ experience opposite magnetic fields $\boldsymbol{B} = -\tau B\hat{z}$, chosen to model the Chern band structure of TBG, and we neglect Zeeman splitting since there is no *real* external magnetic field. In Landau gauge $A_\tau = -\tau B x \hat{y}$, the lowest Landau level (LLL) wave functions are $\phi_{k\tau}(\boldsymbol{r}) \propto e^{iky} e^{-(x-\tau k)^2/2}$, which are created by $c^\dagger_{k\tau\sigma}$. We take $\ell_B \equiv (\hbar/eB)^{1/2} = 1$ throughout. The projected LLL Hamiltonian is [12]

$$
\hat{H} = \frac{1}{2} \sum_{\substack{kpq \\ \tau\tau'\sigma\sigma'}} V_{\tau\tau'}(k,p,q) c^\dagger_{k+q,\tau\sigma} c^\dagger_{k+p-q,\tau'\sigma'} c_{k+p,\tau'\sigma'} c_{k,\tau\sigma}
$$
$$
- \sum_{kp\tau\sigma} V_{\tau+}(k,p,0) c^\dagger_{k\tau\sigma} c_{k\tau\sigma} + \text{const}, \quad (1)
$$

where the second line is a uniform background charge (equivalent to a filled $\tau = +$ LL), and $U(r) = e^2/r$ describes Coulomb interactions with LLL matrix elements $V_{\tau\tau'}(k,p,q) \equiv \langle k+q,\tau; k+p-q,\tau' | \hat{U} | k,\tau; k+p,\tau' \rangle$. The form of (1) is motivated by TBG, where interactions have SU(2) spin rotation invariance and the suppressed intervalley scattering contributions are neglected [6].

We consider a uniform fully spin- and valley-polarized ground state, assuming without loss of generality that $(\tau, \sigma) = (+, \uparrow)$, viz. $|G\rangle \equiv \prod_k c^\dagger_{k+\uparrow} |\text{vac}\rangle$. The scenario with three filled flavors is equivalent via PH conjugation. Following Ref. [12], we compute the collective mode spectrum in the time-dependent Hartree-Fock approximation (TDHFA, equivalent to the generalized random phase approximation [13]). To do so, we solve the dynamics restricted to the basis of single PH pairs, created by the neutral operators $b^\dagger_{\tau\sigma}(k,q) \equiv c^\dagger_{k+q,\tau\sigma} c_{k,+\uparrow}$ (where q is the momentum transfer) that satisfy the equation of motion

$$
-i\partial_t b^\dagger_{\tau\sigma}(k,q) = [\epsilon^{\mathrm{HF}}_{\tau\sigma}(k+q) - \epsilon^{\mathrm{HF}}_{+\uparrow}(k)] b^\dagger_{\tau\sigma}(k,q)
$$
$$
- \sum_{k'} V_{\tau+}(k+q, k'-k-q, k'-k) b^\dagger_{\tau\sigma}(k',q),
$$
$$(2)$$

where $(\tau, \sigma) \neq (+, \uparrow)$, and the k-independent Hartree-Fock (HF) energies are $\epsilon^{\mathrm{HF}}_{\tau\sigma} = -\delta_{\sigma\uparrow}\delta_{\tau+} \sum_p V_{++}(\cdot, p, p)$. Equation (2) is closed for a given τ, σ, and q as these are conserved by the Hamiltonian. Thus, TDHFA is *exact* for the one PH subspace when we neglect LL mixing.

We solve (2) by finding operators $\gamma^\dagger_{\tau\sigma}(q) = \int dk \psi_{q\tau\sigma}(k) b^\dagger_{\tau\sigma}(k,q)$ such that to leading order in $\gamma_{\tau\sigma}(q)$ $[\hat{H}, \gamma^\dagger_{q\tau\sigma}(k)] = \omega_{\tau\sigma}(q) \gamma^\dagger_{q\tau\sigma}(k)$, where $\omega_{\tau\sigma}(q)$ is the excitation energy. The coefficients $\psi_{q\tau\sigma}(k)$ satisfy

$$
[U^{\mathrm{HF}} - \omega_{\tau\sigma}(q)] \psi_{q\tau\sigma}(k) = \int dk' T_{q,\tau}(k,k') \psi_{q\tau\sigma}(k'), \quad (3)
$$

with kernel $T_{q,\tau}(k,k') = (L_y/2\pi) V_{\tau+}(k'+q, k-k'-q, k-k')$, where $U^{\mathrm{HF}} = \sqrt{\pi/2}(e^2/\ell_B)$. Discretizing Eq. (3) yields a 1D hopping problem for each q, with matrix element $T_{q,\tau}(k,k')$ between sites k, k'.

Intravalley spin-wave mode.—For $(\tau, \sigma) = (+, \downarrow)$ and fixed q, the hopping kernel $T_{q,\tau}(k,k')$ depends only on $k - k'$. With the ansatz $\psi_{q\tau\sigma}(k) \sim e^{ik\alpha}$ [12], the energy of this spin-wave collective mode is given by [9,10]

$$
\omega_{+\downarrow}(q,\alpha) = U^{\mathrm{HF}} - \int dk e^{ik\alpha} V_{++}(\cdot, k-q, k), \quad (4)
$$

plotted in Fig. 1(a). The dispersion is isotropic in the (q, α) plane, and α can be interpreted as the x momentum [12]. $\omega_{+\downarrow}(q)$ is gapless and quadratic for $q \to 0$ [9,10,14] and as $q \to \infty$ it saturates to U^{HF} (the loss of exchange energy in creating a hole) since in this limit electron and hole are sufficiently distant that their Coulomb energy vanishes.

Intervalley exciton mode.—A more interesting case is that of intervalley excitations where $\tau = -$. The spectrum is spin independent since $\hat{H}$ is SU(2) symmetric. In fact, the spectrum $\omega_{-\sigma}(q)$ is also independent of q, and hence macroscopically degenerate—a consequence of the "shift symmetry" of the kernel, $T_{q,-}(k,k') = T_{q+2\delta,-}(k-\delta, k'-\delta)$ [15], where increasing q by δ corresponds to shifting the effective 1D hopping problem by $-\delta/2$. The sign and the factor of 2 is strongly suggestive of the notion that $b^\dagger_{\tau\sigma}(k,q)$ creates an excitation that couples to the magnetic field with an effective strength $2eB$ (recall the position-momentum locking of LLs, $\langle x \rangle = \tau k l_B^2$). This leads to a discrete q-independent spectrum of excitonic bound states [Fig. 1(a)] described by harmonic oscillator

wave functions $\psi_{q\tau\sigma}(k;n) \propto H_n\{\sqrt{2}[k+(q/2)]\}e^{-[k+(q/2)]^2}$ centered at $-q/2$, where H_n is a Hermite polynomial corresponding to LLs in an effective magnetic field $2B$.

For rotationally invariant interactions we can capture key features of the excitons [11,15] by working in symmetric gauge and performing a PH transformation on the $\tau = +$ valley, yielding a two-body Hamiltonian for the $+$ hole and $-$ electron. The CM sector is a LLL problem for a charge $-2e$ particle in $-B\hat{z}$, yielding a macroscopic degeneracy $N_{\mathrm{exc}} = 2N_\Phi$ of each valley-flip level due to the doubled coupling to the field. The relative motion corresponds to a charge $-e/2$ particle in the same field and a Coulomb central potential. Solving this in terms of Haldane pseudopotentials [18] yields discrete exciton binding energies $E_m = -(e^2/\ell_B)[\Gamma(m+\frac{1}{2})/2\Gamma(m+1)]$ (where $m \geq 0$ is an integer and Γ is the gamma function), in agreement with numerical solution of Eq. (3). The exciton is a composite neutral object which sees an effectively doubled magnetic field, and whose CM and relative motion are topologically nontrivial (due to Landau quantization) for any interaction. Semiclassical quantization also gives a macroscopic CM degeneracy and discrete relative energy levels, because of the Lorentz-force deflection of electrons and holes as they attract in opposing magnetic fields. In contrast, for the usual case of identical fields the CM of the PH pair evolves in zero field and its energy is nondegenerate [19].

Perturbations away from the LL limit.—We are interested in studying Chern bands with small but nonzero dispersion and nonuniform Berry curvature. To model effects of the single-particle dispersion in our LL model, we transform to the magnetic Bloch basis indexed by two-dimensional momenta k in the magnetic BZ. Picking a square unit cell with side $a = \sqrt{2\pi}$ enclosing unit flux (for magic-angle TBG with $a \simeq 14$ nm, this corresponds to $B \simeq 5$ T), the single-particle magnetic Bloch operators are [6] $d_{k\tau}^\dagger = \frac{1}{\sqrt{N_x}}\sum_{n=0}^{N_x-1} e^{i\tau k_x(k_y+nQ)}c_{k_y+nQ,\tau}^\dagger$ where $Q = 2\pi/a$ is the BZ length and the spin index has been dropped as we are focusing on intervalley modes. Following Ref. [6] we introduce a potential $V(r) = -w[\cos(2\pi x/a) + \cos(2\pi y/a)]$, which is diagonal in this basis and projects to a single-particle dispersion $\epsilon_k = -we^{-\pi/2}(\cos k_x a + \cos k_y a)$ in the LL. Solving the discretized TDHFA equations, we find that exciton energies evolve with the CM momenta q, forming bands within the BZ [Fig. 1(c)]. The topology of exciton bands is encoded in their Berry curvature [3], as we now summarize [15]. The exciton state is [20]

$$|\psi_q^{\mathrm{exc}}\rangle = \sum_k \psi_q(k)d_{k+(q/2),-}^\dagger d_{k-(q/2),+}|G\rangle. \quad (5)$$

After PH transforming the $+$ valley, we can write

$$|u_q^{\mathrm{exc}}\rangle = e^{-iq\hat{R}}\sum_k \psi_q(k)|\phi_{k+(q/2),-}\rangle|\phi_{k-(q/2),+}^*\rangle, \quad (6)$$

where $|\phi_{k,\tau}\rangle$ are the single-particle Bloch states, and the $e^{-iq\hat{R}}$ prefactor ensures that the cell-periodic part $|u_q^{\mathrm{exc}}\rangle$ of $|\psi_q^{\mathrm{exc}}\rangle$ satisfies q-independent boundary conditions [21]. The Berry connection and gauge-invariant Berry curvature are then computed from $|u_q^{\mathrm{exc}}\rangle$. If $a^\tau = i\langle u_q^\tau|\nabla_q|u_q^\tau\rangle$ and $f^\tau = \nabla_q \times a_\tau(q)$ are the Berry connection and curvature of the underlying single-particle bands, the exciton Berry curvature takes the form

$$\Omega_{\mathrm{exc}}(q) = \Omega_{\mathrm{sp}}(q) + \Omega_e(q) + \Omega_{\mathrm{sp},e}(q), \quad (7)$$

where (defining $k_\pm = k \pm \frac{q}{2}$) the first contribution

$$\Omega_{\mathrm{sp}}(q) = \frac{i}{4}\sum_k |\psi_q(k)|^2\{f^+(k_-) - f^-(k_+)\} \quad (8)$$

stems from the single-particle Berry curvature,

$$\Omega_e(q) = i\sum_k \partial_{q_x}\psi_q(k)\partial_{q_y}\psi_q^*(k) - \partial_{q_y}\psi_q(k)\partial_{q_x}\psi_q^*(k) \quad (9)$$

captures the BZ evolution of the envelope function, and

$$\Omega_{\mathrm{sp},e}(q) = \frac{i}{2}\sum_{k,\tau=\pm}\{\partial_{q_y}|\psi_q(k)|^2 a_x^{-\tau}(k_\tau) - (x \leftrightarrow y)\} \quad (10)$$

describes the coupling between the envelope function and the single-particle Berry connection. [Because of the ambiguity in defining a and the phase of $\psi_k(q)$, only the combination $\Omega_e + \Omega_{\mathrm{sp},e}$ is gauge invariant.] Numerically $\Omega_{\mathrm{exc}}(q)$ is computed on a finite k mesh by computing gauge-invariant (non-Abelian) lattice field strengths [22]. Integrating $\Omega_{\mathrm{exc}}(q)$ over the BZ gives a quantized exciton Chern number $C_{\mathrm{exc}} = \int_{\mathrm{BZ}}(d^2q/2\pi)\Omega_{\mathrm{exc}}(q)$.

Armed with this definition we return to our discussion of perturbing the solvable limit. At $w = 0$ the bands are flat and twofold degenerate [23], consistent with the CM experiencing a doubled effective field. As the bandwidth is increased, the upper levels merge into a continuum, which engulfs additional bands as w grows [Fig. 1(c)]. At large enough w the lowest exciton band dips below $E = 0$, signaling an instability to a partially polarized state at the one-exciton level. We also introduce Berry curvature inhomogeneity by artificially deforming the Landau gauge states [15], and find that this leads to a weak exciton dispersion but preserves the Chern numbers. These results illustrate that the exciton dispersion arises from the interplay of the underlying band geometry, topology, dispersion, and interactions. We have also explicitly verified that low-lying exciton bands remain topological with $C_{\mathrm{exc}} = 1$ under these perturbations, even as they acquire dispersion and Berry curvature fluctuations of their own.

Microscopic calculation in TBG.—We now turn to spin and valley-flip excitons of h-BN TBG, for which our

starting point is the continuum model of Ref. [24] with twist $\theta \simeq 1.2°$ lying in the magic-angle regime. We choose the interlayer couplings $w_{AA} = 0.08$ eV and $w_{AB} = 0.11$ eV to account for lattice relaxation effects [25,26]. The h-BN alignment is introduced via a sublattice splitting $|\Delta| = 20$ meV on the bottom layer. We use a dual-gate screened interaction $EU(q) = (e^2/2\epsilon\epsilon_0 q) \tanh(q d_{sc})$ with relative permittivity $\epsilon = 9.5$ and screening length $d_{sc} = 40$ nm [27], and account for interaction double-counting by measuring the density relative to that of decoupled graphene sheets at charge neutrality [15,28]. Projecting to the eight central bands for simplicity, we calculate the fully flavor-polarized self-consistent QAH state at the experimentally relevant filling $\nu = +3$ [8], from which we compute the single valley-flip or spin-flip excitonic spectra in Fig. 2(a) [15]. Consistent with previous studies that focused on energetics [14,29], we find that the spin-flip mode is gapless and disperses quadratically at zero momentum, while the valley-flip mode is gapped. The energetic separation and narrow bandwidth $\simeq 1$ meV of the lowest valley-flip exciton band [Fig. 2(c)] is promising for flat-band physics.

For the above parameters, we find that the lowest two exciton bands have $C_{exc} = 0$. We emphasize, however, that the physics of TBG shows large sample-to-sample variations sensitive to the precise device parameters and experimental conditions. Indeed, by varying the substrate strength, we can induce a set of band touching events which renders the lowest exciton band topological [Figs. 2(b) and 2(d)]. This reveals that the different terms in Eq. (7) can give competing contributions to the exciton Berry curvature. Specifically, the nontrivial structure of the envelope

function $\psi_q(k)$ can render exciton bands trivial even if the underlying single-particle bands have equal and opposite Chern numbers and yield a nonzero gauge-invariant $\Omega_{sp}(q)$. Despite these subtleties, it seems likely that h-BN TBG and other spontaneous QAH systems can host low-lying topological exciton branches in realistic parameter regimes.

Discussion.—We have studied the properties of excitons constituted of particles and holes from bands with equal and opposite Chern numbers, focusing on the Berry curvature experienced by the exciton center-of-mass momentum as it evolves across the BZ. We first studied a solvable model and then showed that universal features are stable to including finite dispersion and Berry curvature inhomogeneities. Using these insights, we analyzed the topology of the low-lying exciton dispersion in h-BN TBG. For realistic interactions we find substantial exciton Berry curvature, integrating to a nonzero Chern number for the lowest exciton band in a subset of the explored parameter space.

As with other topological collective modes [30–32], a nonzero Chern number for a bulk exciton band indicates the presence of chiral exciton modes [33–35] localized at the boundary of the QAH domain, traversing the bulk gap to connect the band to one with a distinct Chern number. These modes allow unidirectional exciton transport, acting as chiral channels for valley charge, but only emerge in TBG for a narrow range of parameters. However, even when the lowest exciton band has $C_{exc} = 0$, we nevertheless find substantial curvature inherited from the underlying Chern bands [Fig. 2(c)]. This can drive anomalous exciton transport in the bulk [3,5]. Each valley-flip exciton of QAH systems such as h-BN TBG is associated with a $U(1)$ valley charge. Since the latter is to very good
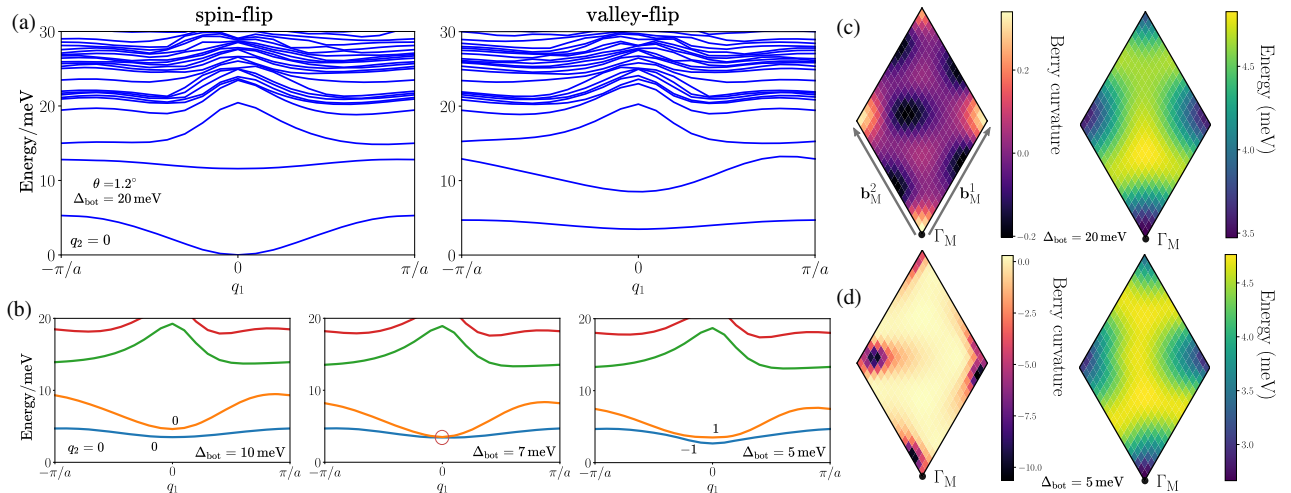

FIG. 2. (a) Spin- and valley-flip exciton spectrum of $\nu = +3$ QAH state of TBG using the continuum model [24], shown along the K_M-Γ_M-K_M line in the moiré BZ. (b) As substrate potential is varied, intervalley exciton bands cross at Γ_M in a topological transition where the Chern numbers of the lowest bands change as indicated with $|\Delta C_{exc}| = 1$. (c) Berry curvature (multiplied by the moiré BZ area) and exciton energy for the lowest valley-flip band of (a) in the moiré BZ. The origin Γ_M and the reciprocal lattice vectors $\mathbf{b}_M^{1(2)} = \sqrt{3} k_\theta (\pm 1/2, \sqrt{3}/2)$ are indicated, where the moiré wave vector $k_\theta = (8\pi/3\sqrt{3}a) \sin\frac{\theta}{2}$. (d) Same as (c) but for the $C_{exc} = -1$ band of the final panel of (b). System size is 20×20.

approximation conserved in these systems, excitons are likely long-lived. Direct optical addressing of these excitons is challenged by the momentum mismatch between the valleys; however, it may be possible to supply this "missing momentum" from another source, e.g., phonons [36]. As conserved bosons in a flat topological band, these valley-flip excitons are a potential platform for engineering neutral bosonic quantum Hall states, a question that we address in a companion work [11].

---

[*]yves.kwan@physics.ox.ac.uk

[1] A. Srivastava and A. Imamoğlu, Phys. Rev. Lett. **115,** 166802 (2015).
[2] J. Zhou, W.-Y. Shan, W. Yao, and D. Xiao, Phys. Rev. Lett. **115,** 166803 (2015).
[3] W. Yao and Q. Niu, Phys. Rev. Lett. **101,** 106401 (2008).
[4] G. Wang, A. Chernikov, M. M. Glazov, T. F. Heinz, X. Marie, T. Amand, and B. Urbaszek, Rev. Mod. Phys. **90,** 021001 (2018).
[5] M. Onga, Y. Zhang, T. Ideue, and Y. Iwasa, Nat. Mater. **16,** 1193 (2017).
[6] N. Bultinck, S. Chatterjee, and M. P. Zaletel, Phys. Rev. Lett. **124,** 166601 (2020).
[7] Y.-H. Zhang, D. Mao, and T. Senthil, Phys. Rev. Research **1,** 033126 (2019).
[8] M. Serlin, C. L. Tschirhart, H. Polshyn, Y. Zhang, J. Zhu, K. Watanabe, T. Taniguchi, L. Balents, and A. F. Young, Science **367,** 900 (2020).
[9] Y. A. Bychkov, S. V. Iordanskiĭ, and G. M. Éliashberg, Sov. J. Exp. Theor. Phys. Lett. **33,** 143 (1981).
[10] C. Kallin and B. I. Halperin, Phys. Rev. B **30,** 5655 (1984).
[11] Y. H. Kwan, Y. Hu, S. H. Simon, and S. A. Parameswaran, arXiv:2003.11559.
[12] A. Karlhede, K. Lejnell, and S. L. Sondhi, Phys. Rev. B **60,** 15948 (1999).
[13] P. Nozieres and D. Pines, *Theory Of Quantum Liquids, Advanced Books Classics* (Avalon Publishing, New York, 1999).
[14] Y. Alavirad and J. Sau, Phys. Rev. B **102,** 235123 (2020).
[15] See Supplemental Material at http://link.aps.org/supplemental/10.1103/PhysRevLett.126.137601 for additional details of theoretical analyses and numerical calculations, which includes Refs. [16,17].
[16] Y. H. Kwan, G. Wagner, N. Chakraborty, S. H. Simon, and S. A. Parameswaran, arXiv:2007.07903.
[17] P. Ring and P. Schuck, *The Nuclear Many-Body Problem* (Springer Science & Business Media, New York, 2004).
[18] F. D. M. Haldane, Phys. Rev. Lett. **51,** 605 (1983).
[19] L. P. Gor'kov and I. E. Dzyaloshinskiĭ, Sov. J. Exp. Theor. Phys. **26,** 449 (1968).
[20] The decomposition of the momenta into $k \pm \frac{q}{2}$ is required to properly decouple the relative and CM sectors.
[21] R. Resta, J. Phys. Condens. Matter **12,** R107 (2000).
[22] T. Fukui, Y. Hatsugai, and H. Suzuki, J. Phys. Soc. Jpn. **74,** 1674 (2005).
[23] For the simple cosine potential considered here, each pair of bands never fully detaches because $\epsilon_k = \epsilon_{-k}$.
[24] R. Bistritzer and A. H. MacDonald, Proc. Natl. Acad. Sci. U.S.A. **108,** 12233 (2011).
[25] N. N. T. Nam and M. Koshino, Phys. Rev. B **96,** 075311 (2017).
[26] S. Carr, S. Fang, Z. Zhu, and E. Kaxiras, Phys. Rev. Research **1,** 013001 (2019).
[27] N. Bultinck, E. Khalaf, S. Liu, S. Chatterjee, A. Vishwanath, and M. P. Zaletel, Phys. Rev. X **10,** 031034 (2020).
[28] M. Xie and A. H. MacDonald, Phys. Rev. Lett. **124,** 097601 (2020).
[29] F. Wu and S. D. Sarma, Phys. Rev. Lett. **124,** 046403 (2020).
[30] R. Shindou, R. Matsumoto, S. Murakami, and J.-I. Ohe, Phys. Rev. B **87,** 174427 (2013).
[31] T. Karzig, C.-E. Bardyn, N. H. Lindner, and G. Refael, Phys. Rev. X **5,** 031001 (2015).
[32] A. V. Nalitov, D. D. Solnyshkov, and G. Malpuech, Phys. Rev. Lett. **114,** 116401 (2015).
[33] F. Wu, T. Lovorn, and A. H. MacDonald, Phys. Rev. Lett. **118,** 147401 (2017).
[34] Z. Gong, W. Luo, Z. Jiang, and H. Fu, Sci. Rep. **7,** 42390 (2017).
[35] K. Chen and R. Shindou, Phys. Rev. B **96,** 161101(R) (2017).
[36] I. V. Kukushkin, J. H. Smet, V. W. Scarola, V. Umansky, and K. von Klitzing, Science **324,** 1044 (2009).